JOURNAL OF CATALYSIS 119, 47–64 (1989)

Effects of High-Temperature Oxidation and Reduction on the Structure and Activity of Rh/Al_2O_3 and Rh/SiO_2 Catalysts

CHOR WONG AND ROBERT W. MCCABE

Physical Chemistry Department, General Motors Research Laboratories, Warren, Michigan 48090-9055

Received December 14, 1988; revised April 14, 1989

The effects of high-temperature oxidizing and reducing treatments on the structure and activity of Rh/Al_2O_3 and Rh/SiO_2 catalysts were examined using the techniques of temperature-programmed reduction, H_2 chemisorption, infrared spectroscopy, transmission electron microscopy, and CO oxidation kinetic analysis. Sequential treatments in O_2 and H_2 at 1075 K had little effect on the Rh/SiO_2 catalysts beyond increasing the mean particle size from ≈4 nm to greater than 12 nm. No interactions between the Rh and the support were observed for the Rh/SiO_2 catalysts. In contrast, 1075 K oxidation of the Rh/Al_2O_3 catalysts caused most of the Rh to diffuse into the bulk of the alumina and resulted in a five- to tenfold decrease in CO oxidation activity. Nearly all of the Rh could be restored to the surface of the alumina by a subsequent 1075-K 1-h H_2 reduction followed by a reoxidation at 775 K for 1 h. The reactivated catalyst oxidized CO at greater rates than the fresh catalyst and with an apparent activation energy of ≈22 kcal/g mol compared to ≈30 kcal/g mol for the fresh catalyst. The data suggest that the most active form of Rh in the reactivated catalyst is small clusters whereas most of the active Rh in the fresh catalyst is present in larger Rh particles which are more bulk-like in character.

INTRODUCTION

Deactivation of automotive exhaust catalysts is of considerable importance due to the high cost and limited availability of the noble metal components. Of primary concern is the deactivation of rhodium which is the principal catalytic component for NO reduction (*1–5*), and which is also effective in catalyzing CO oxidation (particularly during catalyst warmup (*6*)). Rh deactivation is most pronounced in high-temperature oxidizing environments, as pointed out in the review by Taylor (*7*).

Despite the general recognition that high-temperature oxidizing environments are detrimental to Rh-containing catalysts, a detailed understanding of the deactivation mechanism has not emerged. A number of studies have suggested that Rh interacts strongly with γ-Al_2O_3 in oxidizing environments at temperatures above 873 K, even to the extent of forming compounds with, or diffusing below the surface of, the alumina (*4, 8–11*). Other proposed deactivation mechanisms include the formation of difficult-to-reduce oxides of Rh, sintering of Rh to form large particles, and segregation of Rh to the surface of bimetallic Pt–Rh particles with subsequent oxidation of the Rh (*1, 2, 12–14*).

Reactivation of high-temperature oxidized Rh-containing exhaust catalysts is also an issue which has received attention. A number of studies have indicated that high-temperature oxidized Rh catalysts are difficult to reduce and reactivate (*8, 10, 11, 15, 16*). Yao *et al.* (*8*), for example, found that Rh/γ-Al_2O_3 catalysts that had been oxidized above 873 K could be only partially reduced in H_2 at temperatures above 823 K. Similarly, Williams (*5*) and Summers *et al.* (*4, 15*) found that the activities of high-temperature oxidized Rh-containing catalysts could be partially restored after exposure to reducing environments at temperatures of 873 K or higher.

The present study uses a host of techniques to characterize Rh/SiO_2 and Rh/Al_2O_3 catalysts after exposure to high-temperature oxidizing and reducing environments. Although the principal focus is

0021-9517/89 $3.00

on Rh/Al_2O_3 since γ-Al_2O_3 is the main support component in automotive exhaust catalysts, parallel experiments have also been carried out on Rh/SiO_2. We have previously shown that silica does not interact with Rh (*17*); thus a comparison of Rh/SiO_2 data with Rh/Al_2O_3 offers a convenient method of identifying characteristics of the Rh/Al_2O_3 catalyst that are attributable to interactions between the Rh and the alumina.

EXPERIMENTAL

Catalyst Preparation

The SiO_2-supported catalyst was prepared by ion exchange of Davison 923 silica (100–200 mesh, 359 m^2/g BET. area) with rhodium hexammine from aqueous solution to produce a 1% Rh loading. The catalyst was dried in air, reduced in flowing 5% H_2/Ar at 575 K for 2 h, and calcined at 675 K in flowing 5% O_2/He for 1 h prior to use.

The Al_2O_3-supported catalyst was prepared by impregnating γ-Al_2O_3 beads (W. R. Grace) which had been calcined in air at 1175 K to obtain a BET area of 145 m^2/g prior to impregnation. Ion exchange of Rh hexammine from aqueous solution was employed to provide a 0.5% Rh loading. The catalyst was dried, calcined in flowing air at 775 K for 2 h, and crushed into powder prior to use.

The Rh/Al_2O_3 catalyst that was utilized in the high-voltage electron microscope experiments was prepared by a different technique in order to produce Rh particles larger than 5 nm which could be observed in the environmental stage. Both the characterization samples and the microscopy samples utilized the same γ-Al_2O_3. The microscopy samples were prepared by first crushing γ-Al_2O_3 beads and ultrasonically dispersing the Al_2O_3 powder in methanol. The dispersed powder was then deposited on silicon monoxide-coated copper TEM grids, dried overnight at 375 K, and coated with two monolayer-equivalents of Rh by evaporating Rh wire from a tungsten filament in a vacuum coater.

Catalyst Pretreatments

The Rh catalysts prepared by the methods outlined above are referred to as "fresh" catalysts in this report. In most cases, samples of the fresh catalyst were subjected to additional pretreatment prior to use. Samples of both the SiO_2- and Al_2O_3-supported catalysts were treated at high temperatures (1075 K) in oxidizing and reducing environments in order to simulate conditions experienced by automotive exhaust catalysts. Samples that were oxidized in flowing 5% O_2/He for 1 h at 1075 K are designated HTO for high-temperature oxidized, while those that were reduced in flowing 5% H_2/Ar for 1 h at 1075 K are designated HTR for high-temperature reduced. A portion of the HTO catalyst was subsequently given a 1075 K reduction (HTO–HTR), and a portion of the HTO–HTR catalyst was reoxidized in flowing 5% O_2/He at 775 K (HTO–HTR–RO). The latter treatment was used primarily to restore the catalyst to an oxidized form where it could be analyzed by temperature-programmed reduction (TPR). The nomenclature and pretreatment conditions for the Rh/SiO_2 and Rh/Al_2O_3 catalysts are summarized in Table 1.

H_2 Chemisorption

The apparent Rh dispersion of each catalyst was determined by static H_2 chemisorption in a Micromeritics Chemisorb 2800 automated chemisorption analyzer. The

TABLE 1

Summary of Pretreatments

Pretreatment	Rh/SiO_2	Rh/Al_2O_3
Fresh	675 K, 5% O_2	775 K, 5% O_2
HTO	1075 K, 5% O_2	1075 K, 5% O_2
HTR	1075 K, 5% H_2	1075 K, 5% H_2
HTO–HTR	1075 K, 5% O_2	1075 K, 5% O_2
	1075 K, 5% H_2	1075 K, 5% H_2
HTO–HTR–RO	1075 K, 5% O_2	1075 K, 5% O_2
	1075 K, 5% H_2	1075 K, 5% H_2
	775 K, 5% O_2	775 K, 5% O_2

ASTM D 3908-82 procedure was used to pretreat the catalyst and to measure H_2 uptakes; this procedure has been described in detail previously (*18*). The sequence of conditioning pretreatments in the chemisorption apparatus was as follows: (1) 5% O_2 at 725 K for 1 h, (2) 5% H_2 at 725 K for 1 h, and (3) evacuation at 10^{-3} mm Hg and 725 K for 2 h. The chemisorption measurements were carried out at 310 K. The overall H_2 uptake was determined first; the sample was then evacuated and redosed with H_2 to measure the reversible H_2 uptake. The irreversible uptake, used for determining the Rh dispersion, was obtained by subtracting the reversible uptake from the total uptake. An H/Rh ratio of 1 was assumed for the dispersion calculations.

The dispersion measurements were used only to provide a rough indication of the fraction of exposed Rh atoms after each pretreatment. We caution that there are many uncertainties involved in applying chemisorption measurements to Rh catalysts including the chemisorption stoichiometry (which may change with pretreatment): the possibility that the fraction-exposed is changed by the preconditioning procedure in the chemisorption apparatus; the possibility that certain types of Rh sites (such as isolated Rh atoms) may not irreversibly adsorb H_2; and the possibility that the fraction-exposed under reaction conditions may be different than that under conditions of the chemisorption measurements. Moreover, chemisorption measurements cannot distinguish between changes in fraction-exposed due to particle growth and those due to interactions of Rh with the support. Thus a high level of uncertainty is associated with interpreting chemisorption results and related parameters such as mean particle sizes and turn-over frequencies.

CO Oxidation Activity

CO oxidation was used as a probe reaction to examine the effects of the high-temperature oxidizing and reducing pretreatments on the activity of both the alumina- and silica-supported Rh catalysts. The samples were pretreated in a tube furnace and transferred through air to a microreactor. Each experiment utilized 100 mg of catalyst and all samples were reduced in the reactor for 1 h in flowing 5% H_2/Ar at 475 K prior to the start of the experiment (TPR confirmed that this prereduction was sufficient to reduce all Rh_2O_3 in the samples to Rh metal). The reaction was carried out in a stoichiometric feed (40 sccm 5% CO/He, 20 sccm 5% O_2/He). The CO feed was passed through a packed bed of Al_2O_3 beads at 475 K to remove metal carbonyl impurities. A UTI model 100C mass spectrometer was employed for gas analysis downstream of the reactor. Calibration measurements for CO, CO_2, and O_2 were made at 375 K. The temperature was increased in 10-K increments and allowed to equilibrate for 5 min before the gas concentrations were recorded (measurements taken as long as 60 min after temperature equilibration showed no further change in the CO concentration). The 10-K temperature increments were changed to 5- and then 3-K increments as "light-off" was approached. Even though data for all levels of CO conversion are shown, only the differential conversion data (CO conversion $< 10\%$) were used in calculating the kinetic parameters.

Temperature-Programmed Reduction

Temperature-programmed reduction was used to measure the extent of Rh oxidation and to characterize the reducibility of the resulting Rh oxide after oxidizing pretreatments at various temperatures. Our TPR apparatus has been described in detail previously (*17*). Oxidizing pretreatments were carried out in the TPR cell in a 10 cm^3/min flow of 5% O_2/He at each pretreatment temperature for 1 h. The samples were then cooled in the flowing 5% O_2/He stream to 175 K before switching to 5% H_2/Ar and starting the temperature-programmed re-

duction. The TPR profiles were obtained by ramping the temperature at 7 K/min and measuring the H_2 uptake with a thermal-conductivity detector. The overall H_2 uptakes were obtained by integrating the TPR profiles and comparing the H_2 uptakes of the catalyst samples with those of CuO and Rh_2O_3 standards.

Transmission Electron Microscopy

In situ changes in Rh morphology during high-temperature oxidation and reduction were examined in a high-voltage electron microscope (HVEM) equipped with an environmental stage at the National Center for Electron Microscopy, Lawrence Berkeley Laboratories. The HVEM was operated at 1500 keV, thus allowing us to examine the catalyst in 30 Torr of flowing gas. Oxidation and reduction cycles paralleling those in the TPR experiments were carried out in the HVEM. The changes in Rh morphology that resulted from the oxidation and reduction cycles were recorded on videotape.

Only Rh particles which were on the edges of the Al_2O_3 were examined in order to minimize contrast effects due to the strongly diffracting Al_2O_3 support. Exposure of the sample to the electron beam was minimized by maintaining the beam on one section of the catalyst and briefly scanning the area of interest at the appropriate time or temperature.

Fourier-Transform Infrared Spectroscopy

Samples of some of the Rh/Al_2O_3 catalysts were pressed into wafers and examined in a Fourier-transform infrared (FTIR) spectrometer using CO as a probe adsorbate. Details of the spectrometer and cell design have been reported elsewhere (*19*). In all cases, the catalyst wafers were reduced in flowing 5% H_2 in the IR cell at 475 K prior to the introduction of CO. The spectra were recorded in flowing CO at 375 K as a function of time.

RESULTS

H_2 Chemisorption

Hydrogen chemisorption results are reported as percentages exposed in Table 2 assuming a 1-to-1 H-atom to surface Rh-atom chemisorption stoichiometry. The percentages exposed were relatively high for the fresh and the HTR Rh/SiO_2 catalysts (35 and 28%, respectively), but decreased to 9% or less for those samples that had received a high-temperature oxidation at some point in their pretreatment schedule. The percentages exposed for fresh and HTR Rh/Al_2O_3 catalysts (33 and 28%, respectively) were nearly identical to those of their silica-supported analogs. High-temperature oxidation of the Rh/Al_2O_3 catalyst also resulted in a sharp drop in the percentage exposed, although not as severe as that of the Rh/SiO_2 catalyst (10% for HTO Rh/Al_2O_3 vs 4% for HTO Rh/SiO_2). The most

TABLE 2

Summary of CO–Oxidation Results

Pretreatment	1% Rh/SiO_2			0.5% Rh/Al_2O_3		
	Percentage Rh exposed	E_a (kcal/mol)	$T_{50\%}$ (K)	Percentage Rh exposed	E_a (kcal/mol)	$T_{50\%}$ (K)
Fresh	35	28.8	436	33	29.6	459
HTO	4	30.2	434	10	26.0	494
HTR	28	28.6	434	28	32.8	452
HTO–HTR	7	28.2	441	21	22.9	480
HTO–HTR–RO	9	29.8	444	29	22.2	452

significant contrast between the alumina- and silica-supported catalysts was in the chemisorption behavior of the HTO catalysts after subsequent HTR treatments. As noted above, the Rh/SiO_2 catalysts remained at percentages exposed of 9% or less even after subsequent HTR treatments. However, the HTO Rh/Al_2O_3 catalysts regained significant chemisorption capacity after subsequent HTR (21%) and HTR–RO (29%) treatments.

CO Oxidation

CO oxidation activity is reported for both the alumina- and silica-supported Rh catalysts in Fig. 1 (as CO conversion vs temperature profiles covering the complete conversion range) and in Fig. 2 (as Arrhenius plots based on data obtained at conversions less than 15%). The most significant feature in both figures is the much broader range of CO oxidation activity observed for the Rh/Al_2O_3 catalyst as a function of pretreatment compared to that of the Rh/SiO_2 catalyst. For the Rh/SiO_2 catalyst, the fresh catalyst was most active, the HTR catalyst showed almost identical activity, and the HTO catalysts were slightly less active. Differences in 50% conversion temperatures were at most 12° (see Table 2) and rates differed by at most a factor of 2. Moreover, apparent activation energies were all 29.2 ± 1 kcal/g mol, independent of pretreatment.

In contrast to Rh/SiO_2, 50% conversion temperatures varied by 42° and rates by as

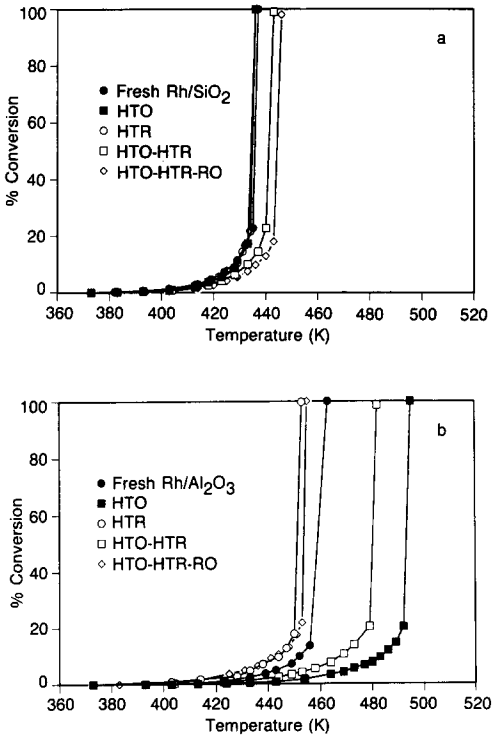

FIG. 1. Plots of percentage CO conversion as a function of steady-state temperature for samples of 1% Rh/SiO_2 catalyst (a) and 0.5% Rh/Al_2O_3 catalyst (b). In each case, curves are shown both for the fresh catalyst and after various reducing and oxidizing treatments (defined in the text). The CO flow rate was 40 sccm and the O_2 flow rate was 20 sccm; 100 mg of catalyst was used in all cases.

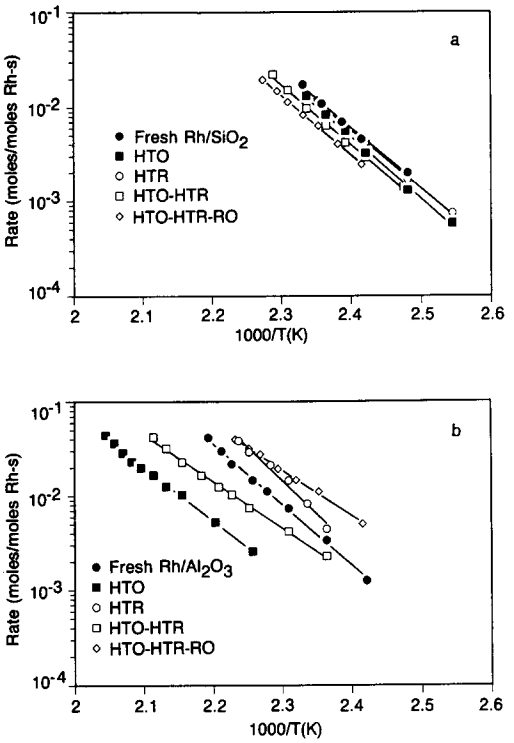

FIG. 2. Arrhenius plots of the CO oxidation rate (moles CO converted per mole Rh per second) for samples of 1% Rh/SiO_2 catalyst (a) and 0.5% Rh/Al_2O_3 (b). Samples are the same as those in Fig. 1 but rates were obtained at conversions less than 15%. Note that the rates are expressed in terms of the total Rh contained in the samples, not the exposed Rh.

much as an order of magnitude over that of the Rh/Al_2O_3 catalyst after the various pretreatments. High-temperature oxidation had the greatest effect on decreasing CO oxidation activity relative to the fresh catalyst activity, while high-temperature reduction increased activity relative to the fresh catalyst activity. High-temperature oxidation, followed by HTR or HTR–RO treatment, resulted in restoration of some or all of the activity lost by high-temperature oxidation. Also in contrast to Rh/SiO_2, the apparent activation energies for CO oxidation over the alumina-supported catalyst varied widely from 22 to 33 kcal/g mol as a function of pretreatment.

Temperature-Programmed Reduction

Our TPR results for the Rh/SiO_2 catalyst have been reported previously (*17*), so only the essential features will be summarized here. Rh/SiO_2 catalysts are completely oxidized to Rh_2O_3 following O_2 exposure at temperatures of 875 K or above (see Fig. 5). After oxidation at 875 K the TPR profile showed peaks at 355 and 450 K as shown in Fig. 3. Oxidation at higher temperatures decreased the area of the 355-K peak and increased the area of the 450-K peak. However, the overall area remained constant and corresponded to the stoichiometric conversion of Rh_2O_3 to Rh metal. The changes in peak areas have been shown to result from changes in Rh particle morphology rather than changes in oxidation state (*17*).

TPR profiles for the Rh/Al_2O_3 catalyst following various pretreatments are presented in Fig. 4. Consistent with the Rh/SiO_2 catalysts, the reduction profile for the 675-K oxidized catalyst contained two poorly resolved peaks at temperatures characteristic of Rh_2O_3 reduction. However, unlike Rh/SiO_2, the integrated area under the TPR profiles decreased with increasing oxidation temperatures, as shown

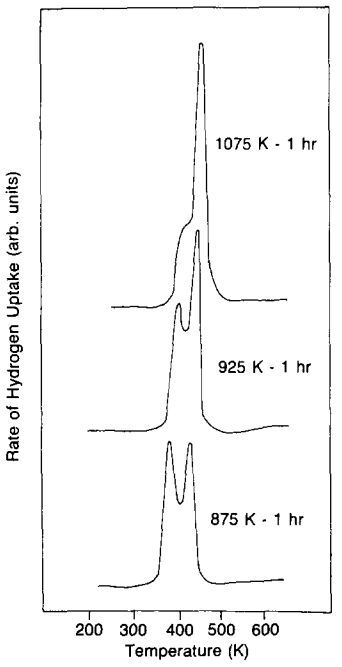

FIG. 3. Temperature-programmed reduction profiles for 1% Rh/SiO_2 expressed as rate of H_2 uptake (arbitrary units) vs temperature. The heating rate was 7 K/min and the flow rate was 10 sccm 5% H_2/Ar. The temperature labels on each reduction profile indicate the temperature of the oxidizing treatment preceding the reduction.

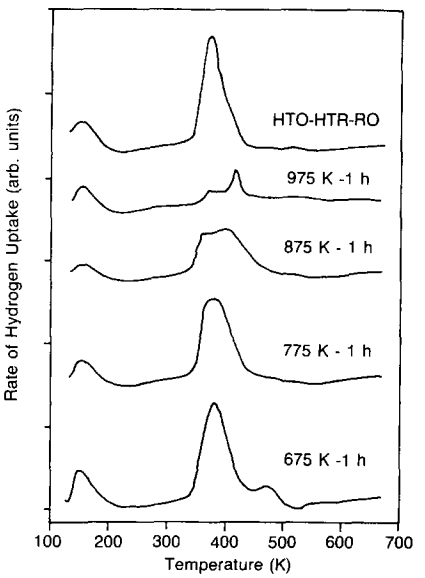

FIG. 4. Temperature-programmed reduction profiles for 0.5% Rh/Al_2O_3. See Fig. 3 legend and text for description.

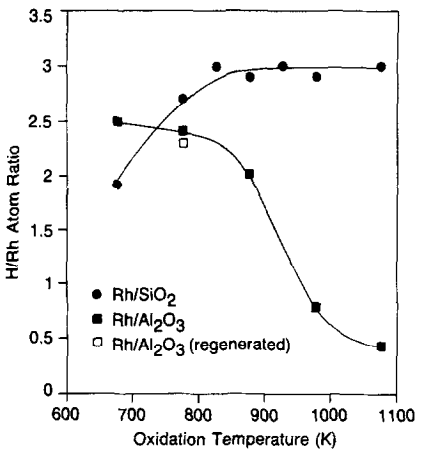

FIG. 5. A plot showing the integrated H_2 uptake in temperature-programmed reduction (expressed as an H-atom to total Rh-atom ratio) as a function of the oxidation temperature preceding the TPR experiment. Data are shown for the 1% Rh/SiO_2 catalyst (solid circles), the 0.5% Rh/Al_2O_3 catalyst (solid squares), and the HTO–HTR–RO Rh/Al_2O_3 catalyst (open square).

in Fig. 5. Only 14% of the Rh oxide underwent the equivalent of a Rh^{3+} to Rh^0 reduction during TPR of the 1075-K (HTO) sample.

The quantity of reducible Rh in an HTO Rh/Al_2O_3 catalyst could be increased by subsequently reducing the sample at 1075 K followed by reoxidizing it at 775 K (HTO–HTR–RO). The TPR profile for the HTO–HTR–RO Rh/Al_2O_3 catalyst (shown in Fig. 4) is nearly identical to that of the fresh catalyst oxidized at 775 K. Furthermore, Fig. 5 shows that nearly identical quantities of H_2 were consumed in reducing the fresh (i.e., 775-K oxidized) and HTO–HTR–RO catalysts.

Transmission Electron Microscopy

TEM was used to study the changes in Rh morphology that occurred as a result of the various pretreatments. Figure 6 shows a section of the model Rh/Al_2O_3 catalyst after oxidation at 775 K (a) and 1025 K (b). Rh particles were clearly visible in the still-plate photographs after heating at 775 K in 5% O_2 but disappeared as the temperature was increased to 1025 K in 5% O_2. (Note that 1025 K, although below our standard HTO temperature of 1075 K, was the highest temperature attainable in the environmental stage on the HVEM.) Subsequent reduction of the Rh/Al_2O_3 at 1025 K resulted in no reappearance of Rh particles in the detectable size range (> 5 nm). No Rh particles disappeared from the surface of the SiO_2-supported catalyst during similar treatments, but the mean Rh particle size increased (*17*).

In a separate experiment, a group of Rh particles was monitored continuously with videotape to observe changes in the immediate vicinity of the $Rh–Al_2O_3$ interface during high-temperature oxidation. Figure 7 shows a sequence of micrographs (derived from the videotape) at various times after switching to 5% O_2 and simultaneously beginning a temperature ramp from 775 to 1025 K (the particles were initially reduced at the start of the experiment). The Rh particles appeared rounded at 775 K (Fig. 7a), but began to form faceted edges as the temperature was ramped through 823 K (Fig. 7b). Most of the Rh disappeared over the course of 40 min at 1025 K (Fig. 7c). Large particles did not reform after heating in 5% H_2 at 1025 K for 40 min (Fig. 7d). Note that the disappearance of the Rh particles in high-temperature oxygen was not due to contrast changes caused by reorientation of the particles; this was confirmed by tilting the sample by ±15°.

Infrared Spectroscopy

FTIR spectra, obtained in flowing CO at 373 K, are shown in Fig. 8a for fresh, HTR, and HTO Rh/Al_2O_3 catalysts. The fresh catalyst contained bands at 2086 and 2014 cm^{-1} corresponding to the stretching frequencies of the CO dicarbonyl species, as well as bands at 2056 cm^{-1} (corresponding to the stretching frequency of linearly adsorbed CO), and at 1850 cm^{-1} (corresponding to the stretching frequency of bridge-bonded CO). The overall integrated absorbance for the CO bands of the fresh catalyst was 18.0 cm^{-1}.

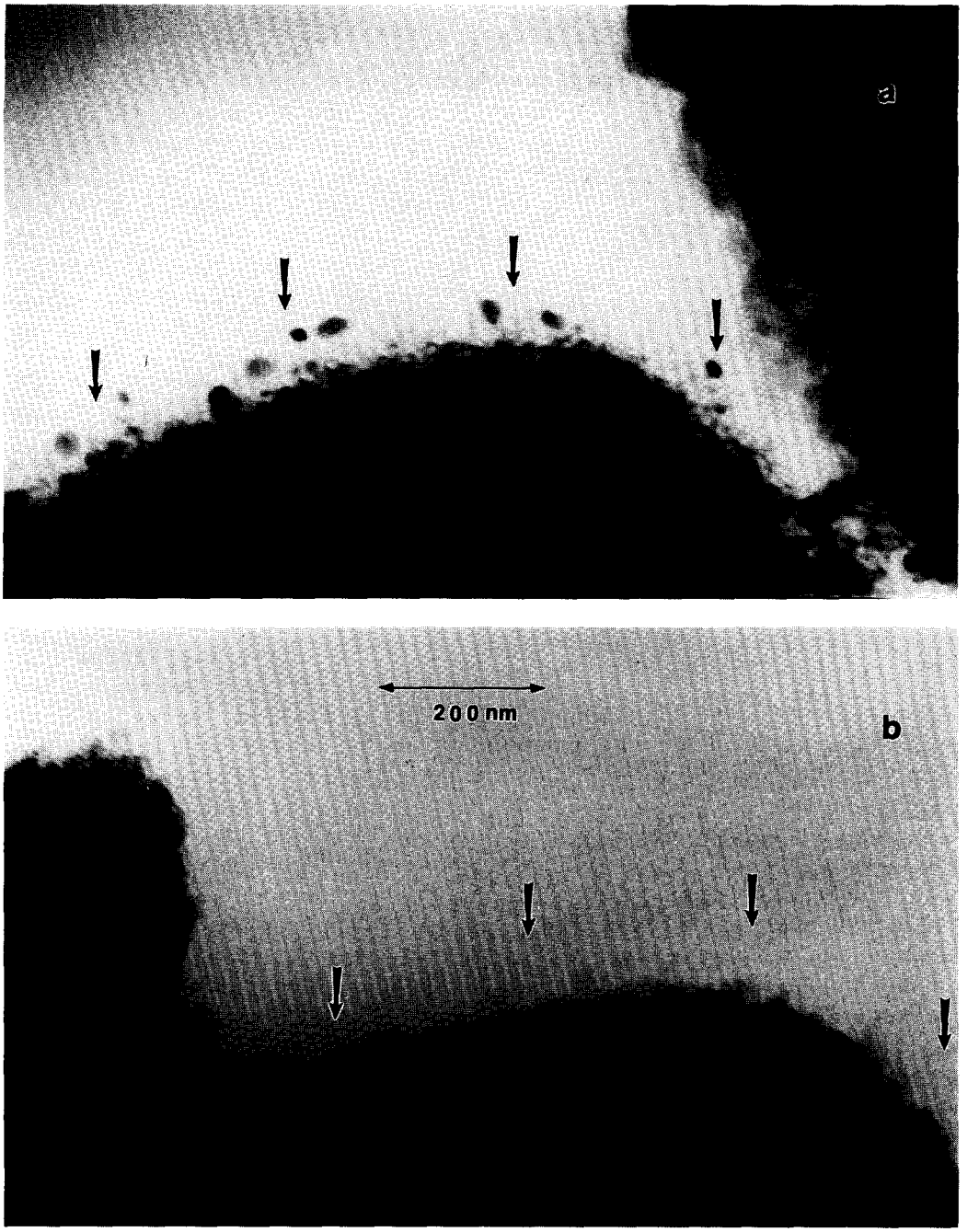

FIG. 6. Electron micrographs (photographic plates) showing the model Rh/Al_2O_3 catalyst after (a) 775-K and (b) 1025-K oxidations in 5% O_2. Note that the plates are shifted horizontally relative to one another, but the arrows denote identical locations in each case.

FIG. 7. A sequence of electron micrographs showing videotape frames of a selected group of Rh particles on the model Rh/Al_2O_3 catalyst during oxidation (a) immediately upon switching from a reducing atmosphere to an oxidizing atmosphere at 775 K, (b) while the catalyst is being ramped through 825 K in 5% O_2, (c) after 40 min in 5% O_2 at 1025 K, and (d) after a subsequent 40 min in 5% H_2 at 1025 K.

FIG. 7—*Continued*

FIG. 7—*Continued*

FIG. 7—*Continued*

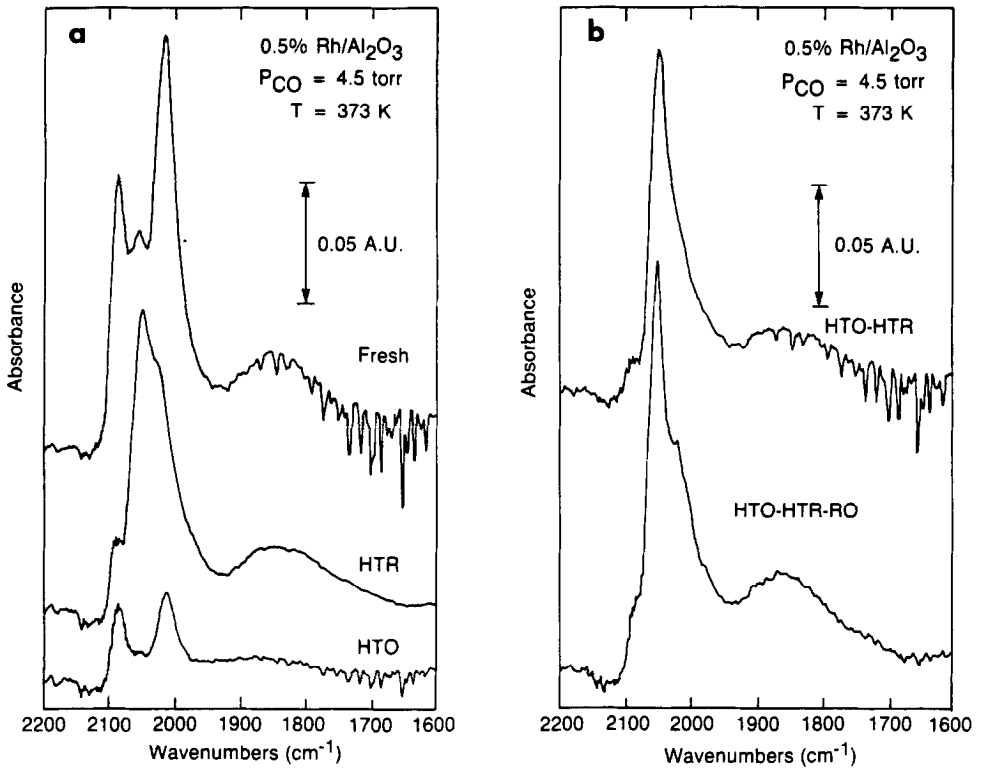

FIG. 8. Fourier-transform infrared spectra of the CO-stretching region obtained for the 0.5% Rh/Al_2O_3 catalyst after various pretreatments: (a) fresh, HTR, and HTO catalysts, (b) HTO–HTR and HTO–HTR–RO catalysts. Fine structure in the spectra below 1750 cm^{-1} is due to incomplete subtraction of background water bands from the support. The spectra were obtained in flowing CO, but the gas phase CO has been subtracted out. Note that all samples were given a standard preconditioning treatment in H_2 at 475 K *in the IR cell* prior to CO exposure at 373 K.

The HTR catalyst showed a sharp decrease in dicarbonyl absorbance compared to that of the fresh catalyst, leaving the linear band as the principal mode. The overall integrated absorbance for the HTR catalyst was 9.2 cm^{-1}.

The principal features associated with the HTO catalyst were a sharp decrease in total absorbance to 3.6 cm^{-1} and almost complete disappearance of the linear and bridge-bonded bands.

Figure 8b shows the corresponding FTIR spectra obtained after high-temperature reductions of the HTO catalyst aimed at restoring lost activity. Both the HTO–HTR and HTO–HTR–RO catalysts showed significant recovery in total absorbance to 11.6 cm^{-1} and 15.1 cm^{-1}, respectively. In contrast to the fresh catalyst, both the HTO–HTR and HTO–HTR–RO catalysts showed predominantly linear and bridged CO rather than dicarbonyl CO. Interestingly, the net effect of the HTO–HTR–RO treatment was to convert the fresh catalyst from a state where the dicarbonyl band predominated to a state where the linear and bridged features predominated without greatly changing the overall CO absorbance.

DISCUSSION

This discussion focuses on the state of the Rh/Al_2O_3 catalyst in its fresh form and after the various high-temperature pretreatments. To this end, Table 3 provides a summary of the principal observations obtained

TABLE 3

Summary of Results for Rh/Al_2O_3

	Catalyst designation				
	Fresh	HTO	HTR	HTO–HTR	HTO–HTR–RO
State of catalyst	• Mostly surface Rh • Both particles and isolated atoms	• Mostly subsurface Rh • Exposed Rh mostly isolated atoms	• Mostly surface Rh • Mostly particles	• Mostly surface or near-surface Rh • Small clusters and larger particles	• Mostly surface Rh • Small clusters and larger particles
	Supporting evidence				
H_2 chemisorption (% Rh-exposed)	33%	10%	28%	21%	29%
CO-oxidation	High activity	Low activity	Slightly greater than fresh	Less than fresh greater than HTO	Slightly greater than fresh
TPR	H/Rh of 2.5	Nearly complete loss of H_2 uptake	(Not applicable)	(Not applicable)	• Similar to fresh • Nearly complete recovery of H_2 uptake
TEM	Most particles less than 5 nm	• Few visible particles • Direct observation of Rh particle disappearance	Most particles less than 5 nm	Most particles less than 5 nm	Some visible particles greater than 5 nm
FTIR with CO[a]	A_i = 18.0 cm^{-1} • Linear, bridged, and dicarbonyl all present	A_i = 3.6 cm^{-1} • Small dicarbonyl features dominate spectrum	A_i = 9.2 cm^{-1} • Linear and bridged features predominate	A_i = 11.6 cm^{-1} • Predominantly linear and bridged features	A_i = 15.1 cm^{-1} • Predominantly linear and bridged features

[a] A_i indicates integrated absorbance.

from each characterization technique after each pretreatment. Based on the combined results of the various characterization techniques, as well as comparison with the Rh/SiO_2 catalyst, we also present in Table 3 a qualitative description of the state of the Rh/Al_2O_3 catalyst at each point in the treatment scheme.

Fresh Rh/Al_2O_3

The TPR H/Rh ratio of 2.5 for the fresh Rh/Al_2O_3 catalyst indicates that nearly all of the Rh is present above the surface of the alumina in a readily reducible form. The slightly lower H/Rh ratio than observed for Rh/SiO_2 (3.0) could be due to a small amount of Rh below the surface of the alumina, and thus inaccessible to O_2 and H_2. Alternatively, some of the Rh may not undergo full conversion from Rh^0 to Rh^{3+} during oxidation and reduction. In particular, isolated Rh atoms (suggested by the dicarbonyl bands in the CO IR spectrum) might not oxidize fully to Rh^{3+} or reduce fully to Rh^0.

H_2 chemisorption suggests a mean particle size near 3.3 nm for the fresh 0.5% Rh/Al_2O_3 catalyst. Relatively small particles are also indicated by the TEM data for the model Rh/Al_2O_3 catalyst, where few particles greater than 5 nm were observed despite a higher local Rh loading than that in the 0.5% Rh/Al_2O_3 catalyst. The presence of bridged, linear, and dicarbonyl features in the CO IR spectrum suggests that the fresh catalyst contains isolated Rh atoms as well as Rh particles.

CO oxidized at a rate of 3.5×10^{-3} mol/mol Rh-s at 425 K, yielding an apparent turnover frequency of 1.1×10^{-2} s^{-1}. This is within a factor of 2 of an extrapolated turnover frequency of 2×10^{-2} s^{-1} at 425 K from data reported by Oh *et al.* (*20*) for a 0.01% Rh/Al_2O_3 catalyst (note that this extrapolated turnover frequency contains a correction for the different O_2/CO ratios employed in the two studies). By way of comparison, the fresh Rh/SiO_2 catalyst yielded an apparent turnover frequency of 3.4×10^{-2} s^{-1}. The apparent activation en-

ergy of 29.6 kcal/g mol for the fresh Rh/Al_2O_3 catalyst is close to the value of 28.8 kcal/g mol obtained for the fresh Rh/SiO_2 catalyst; both values are close to activation energies reported by others for bulk Rh (28–29 kcal/g mol) (*20, 21*), Rh/Al_2O_3 (30 kcal/g mol) (*20*), and Rh/SiO_2 (26.4 kcal/g mol) (*12*).

As summarized in Table 3, the data show that *the fresh catalyst contains nearly all of its Rh above the surface of the alumina distributed as both isolated atoms and particles with mean diameter of ≈3 nm.*

HTO Rh/Al_2O_3

As summarized in Table 3, all of the probes employed in this study point toward a large decrease in exposed Rh atoms after the HTO treatment. On SiO_2, the decrease in the number of exposed Rh atoms is most likely due to the decrease in surface area associated with particle growth under HTO conditions. On Al_2O_3, the decrease in fraction-exposed could be due to either particle growth or to interaction of the Rh with the alumina support. The sharp decrease in TPR uptakes suggests that the latter possibility is more likely, since we have shown on the basis of the Rh/SiO_2 TPR data that even large Rh_2O_3 particles are stoichiometrically reduced to Rh metal at temperatures near 500 K.

The interaction of Rh with the alumina support could involve either subsurface diffusion of Rh cations or the formation of surface complexes between Rh and the alumina. Although the formation of a strongly interacting Rh surface complex cannot be completely ruled out, our data appear to be best explained by a mechanism involving subsurface diffusion of Rh cations under high-temperature oxidizing conditions. In particular, the TPR experiments showed that temperatures above 875 K are required both for oxidative deactivation of the catalyst and subsequent H_2 reactivation. Such high temperatures are required for bulk diffusion of metal cations in oxide matrices (*22–24*). The combined TEM and IR data are also consistent with a deactivation mechanism involving subsurface Rh diffusion. TEM alone cannot distinguish between disappearance of large Rh particles due to diffusion of Rh into the support or due to spreading of Rh_2O_3 over the surface of the alumina and subsequent interaction with the alumina. However, we saw no evidence for thinning and spreading of Rh_2O_3 particles during our *in situ* observations of Rh particle disappearance. Furthermore, our TEM samples initially contained two monolayers of Rh; thus even if a monolayer $Rh–Al_2O_3$ complex had been formed, the remaining Rh could have sintered to form large particles. Few large (>5 nm) Rh particles were observed in our HTO samples and subsequent heating at 1025 K in both O_2 and H_2 for up to 2 h failed to produce visible Rh particles. In keeping with our TEM observations, the strong suppression of all CO vibrational modes seems inconsistent with a surface containing a highly dispersed $Rh–Al_2O_3$ complex since, in that case, shifts in band frequencies or relative changes in band intensities would be expected. Instead, the "disappearance" of CO in IR appears consistent with diffusion of most of the Rh below the surface of the alumina.

The HTO Rh/Al_2O_3 catalyst was the least active of this study, showing an extrapolated rate at 425 K of 6.9×10^{-4} mol/mol Rh-s compared to the corresponding fresh catalyst rate of 3.5×10^{-3} mol/mol Rh-s. Comparison with the HTO Rh/SiO_2 catalyst suggests that the activity loss is not due to particle growth; chemisorption and TEM both showed that the mean Rh particle size on the silica-supported catalyst increased from a fresh value of ≈4 nm to a final value of 12 nm or greater after high-temperature oxidation. Despite the significant particle growth, little change in CO oxidation activity was observed for the Rh/SiO_2 catalyst. The lower apparent activation energy for the HTO Rh/Al_2O_3 catalyst (26.0 kcal/g mol) compared to the HTO Rh/SiO_2 catalyst (30.2 kcal/g mol) also argues against simple particle growth as a deactivation

mechanism for the HTO Rh/Al_2O_3 catalyst. The lower activation energy observed for the HTO Rh/Al_2O_3 catalyst could be indicative of reaction predominantly on isolated Rh atoms, since the dicarbonyl bands, although weak, were the principal IR features observed on the deactivated catalyst.

In summary, *most of the Rh in the HTO Rh/Al_2O_3 catalyst is dissolved in the bulk of the alumina, with small concentrations of isolated Rh atoms and Rh particles remaining above the surface.*

HTR Rh/Al_2O_3

Direct high-temperature reduction of the fresh catalyst resulted in only a slight decrease in apparent dispersion and produced a catalyst with greater activity than the fresh catalyst. Although the overall CO IR absorbance decreased by a factor of 2 compared to the fresh catalyst, virtually all of the loss in absorbance was due to a sharp reduction in the intensity of the dicarbonyl bands. The absorbance in the linear region increased, suggesting that the main effect of the high-temperature reduction was to nucleate Rh particles from isolated Rh atoms. That this process of converting isolated Rh atoms to particles occurs without significant change in H_2 chemisorption is consistent with recent observations by others in our laboratory (*11, 25*) (based on comparisons between CO and H_2 chemisorption) suggesting that isolated Rh atoms do not chemisorb H_2. Thus any loss of surface Rh atoms which may occur by sintering of existing particles is nearly compensated for by the formation of new particles from isolated Rh atoms. The formation of new particles by nucleation of isolated Rh atoms also provides an explanation for the increase in CO oxidation activity, since isolated Rh atoms have been reported to be less active than particulate Rh for CO oxidation (*26*).

Thus we conclude in Table 3 that *virtually all of the Rh in the HTR catalyst is above the surface of the alumina and contained in Rh particles of ≈4 nm mean diameter.* As might be expected, the apparent activation energy for CO oxidation over the HTR catalyst (30–33 kcal/g mol) is high and characteristic of particulate Rh.

HTO–HTR and HTO–HTR–RO Rh/Al_2O_3

The most significant feature of the HTO–HTR and the HTO–HTR–RO catalysts is that they showed recovery of CO oxidation activity compared to the HTO catalyst. This implies that high-temperature heating in H_2 causes Rh to return to the surface of the alumina where they are reduced and trapped as metal particles. The characterization techniques provided additional evidence that Rh returns to the surface of the alumina. Table 3 shows that this process is nearly complete for the HTO–HTR–RO catalyst, as indicated by the return of (1) the chemisorption capacity to 88% of the fresh value, (2) the TPR uptake to 92% of the fresh value, and (3) the integrated CO absorbance to 84% of the fresh value.

Despite the clear indication of catalyst reactivation following the subsequent HTR and HTR–RO treatments of the HTO catalyst, two broad questions remain concerning the states of both the HTO–HTR and the HTO–HTR–RO Rh/Al_2O_3 catalysts. Most significantly, both catalysts retained a "memory" of the HTO treatment in the sense that the apparent CO oxidation activation energy was lower by 8–10 kcal/g mol than that of either the fresh or the HTR catalyst. Thus the first question is "what is the cause of this memory effect?", particularly in the case of the HTO–HTR–RO catalyst, which otherwise is very similar to the fresh and the HTR catalysts. The second question is "why does the HTO–HTR–RO catalyst show markedly higher CO oxidation activity, CO chemisorption capacity, and integrated CO IR absorbance than those of the HTO–HTR catalyst?"

Although we cannot provide definite answers to the above questions, we suggest that the HTO–HTR and HTO–HTR–RO results are consistent with the following scenario. We propose that the HTO–HTR and the HTO–HTR–RO catalysts contain

Rh clusters in addition to larger Rh particles. The inability to detect Rh particles in the HVEM and the appearance of large linear CO absorbance bands in the FTIR suggest that a highly dispersed contiguous form of Rh is present in the HTO–HTR sample. Furthermore, evidence for the existence of a highly dispersed contiguous form of Rh, distinct from both isolated Rh atoms and bulk-like Rh particles, has been widely reported in the literature; this form of Rh has been variously referred to as "dispersed" Rh (*9, 21, 27, 28*), Rh rafts (*29*), Rh platelets (*13, 35*), Rh clusters (*31–34*), and 0.6–1.2-nm Rh particles (*30*). In our scenario, CO oxidation occurs predominantly on the Rh clusters in the HTO–HTR and the HTO–HTR–RO catalysts. The low activation energies would result from different CO or O_2 adsorption properties in the clusters compared to those in larger particles (van Zon *et al.* (*30*) have shown that most of the Rh atoms in 0.6- to 1.2-nm clusters are in direct contact with the support; thus different CO and O_2 adsorption characteristics would be expected for these Rh clusters in close proximity to the alumina compared to those for Rh atoms in a metal matrix). These results are consistent with the lower activation energy for CO oxidation over highly dispersed Rh/Al_2O_3 catalysts observed by Yu Yao (*21*). Thus, the "memory" effect is associated with the formation of stable Rh clusters in both the HTO–HTR and the HTO–HTR–RO samples. Differences in CO oxidation activity, CO IR band intensities, and CO chemisorption uptakes between the HTO–HTR and the HTO–HTR–RO catalysts could simply reflect different distributions of Rh between clusters and large particles in the two catalysts. Lee and Schmidt (*36*) observed an increase in both the Rh dispersion and the ethane hydrogenolysis activity of a Rh/SiO_2 catalyst after the sample had undergone oxidation followed by reduction at 475 K. The enhancement in activity was attributed to the formation of small Rh clusters from large Rh–oxide particles upon low-temperature reduction. Our HTO–HTR–RO sample had undergone a similar final treatment (i.e., oxidation at 775 K followed by a 475-K reduction in the reactor prior to running CO oxidation); thus a similar mechanism may be responsible for the improved CO oxidation activity as well as the higher apparent Rh dispersion.

In summary we conclude that *most of the Rh in the HTO–HTR and HTO–HTR–RO is near or on the surface of the alumina and probably distributed as a mixture of small Rh clusters and larger particles.* Additional studies will be required to obtain a detailed understanding of the active phase in the HTO–HTR and the HTO–HTR–RO catalysts and the mechanism by which it is formed.

SUMMARY

- High-temperature oxidation and reduction of Rh/SiO_2 only sintered the Rh crystallites; no evidence was obtained for interaction between Rh and the SiO_2.
- CO oxidation activity was relatively insensitive to mean particle size on Rh/SiO_2. Particle growth from 4 to 12 nm led to at most a factor of 2 decrease in CO oxidation activity.
- The fresh Rh/Al_2O_3 catalyst contained a mixture of isolated Rh atoms and Rh particles, with CO oxidation occurring principally on the particles.
- The high-temperature reduced (i.e., HTR) catalyst had fewer isolated Rh atoms and greater CO oxidation activity than the fresh catalyst. The apparent activation energy remained near 30 kcal/g mol—characteristic of bulk Rh.
- The high-temperature oxidized (i.e., HTO) Rh/Al_2O_3 catalyst had a CO oxidation rate five times lower than that of the fresh catalyst due to diffusion of most of the Rh into the bulk of the alumina.
- The high-temperature reduced HTO Rh/Al_2O_3 catalyst (i.e., the HTO–HTR catalyst) partly regained the activity lost by the HTO catalyst; the high-temperature re-

duction restored much of the Rh back to the surface of the alumina.

• Reoxidation of the HTO–HTR Rh/Al_2O_3 catalyst at 775 K produced a catalyst (i.e., the HTO–HTR–RO catalyst) with almost as much surface Rh as the fresh catalyst. However, the state of Rh in this catalyst appeared different from that in the fresh catalyst. CO oxidized at higher rates over this catalyst than over the fresh catalyst and with lower activation energy (22 kcal/g mol vs 30 kcal/g mol for the fresh catalyst). These observations suggest that small clusters may constitute the active form of Rh in the regenerated catalyst.

ACKNOWLEDGMENTS

The catalysts were prepared by M. G. Zammit who also carried out the chemisorption analyses. R. A. Dictor provided the IR analyses of the catalysts and also helped with valuable discussions of the data. We also acknowledge the assistance of the staff at the National Center for Electron Microscopy (Lawrence Berkeley Laboratories), particularly D. Ackland.

REFERENCES

1. Koberstein, E., SAE Paper No. 770366 (1977).
2. Cooper, B. J., Harrison, B., Shutt, E., and Lichtenstein, I., SAE Paper No. 770367 (1977).
3. Schlatter, J. C., and Taylor, K. C., *J. Catal.* **49,** 42 (1977).
4. Summers, J. C., Monroe, D. R., Chang, C. C., and Gaarenstroom, S. W., Paper presented at the Materials Research Socity Meeting, Boston, MA (1977). Available as General Motors Research Publication GMR-3147.
5. Williams, F. ., "Pretreatment Effects on the Catalytic Activity and the Oxidation State of Rhodium." General Motors Research Laboratories Report No. PC-55, 1977.
6. Taylor, K. C., *Ind. Eng. Chem. Prod. Res. Dev.* **11,** 54 (1972).
7. Taylor, K. C., "Automotive Catalytic Converters." Springer–Verlag, Berlin, 1984.
8. Yao, H. C., Japar, S., and Shelef, M., *J. Catal.* **50,** 407 (1977).
9. Yao, H. C., Stepien, H. K., and Gandhi, H. S., *J. Catal.* **61,** 547 (1980).
10. Duprez, D., Delahay, G., Abderrahim, H., and Grimblot, J., *J. Chim. Phys.* **83,** 465 (1986).
11. Beck, D. D., and Carr, C. J., submitted for publication.
12. Kiss, J. T., and Gonzalez, R. D., *Ind. Eng. Chem. Prod. Res. Dev.* **24,** 216 (1985).
13. Yates, D. J. C., and Prestridge, E. B., *J. Catal.* **106,** 549 (1987).
14. Fiedorow, R. M. J., Chahar, B. S., and Wanke, S. E., *J. Catal.* **51,** 193 (1978).
15. Summers, J. C., and Ausen, S. A., *J. Catal.* **58,** 131 (1979).
16. Duprez, D., Barrault, J., and Geron, C., *Appl. Catal.* **37,** 105 (1988).
17. Wong, C., and McCabe, R. W., *J. Catal.* **107,** 535 (1987).
18. D'Aniello, M. J., Jr., Monroe, D. R., Carr, C. J., and Krueger, M. H., *J. Catal.* **109,** 407 (1988).
19. Dictor, R. A., and Roberts, S., "The Influence of Ceria on Alumina-Supported Rhodium: Observations of Rhodium Morphology Using FTIR Spectroscopy." General Motors Research Report PC-446, May 1988.
20. Oh, S. H., Fisher, G. B., Carpenter, J. E., and Goodman, D. W., *J. Catal.* **100,** 360 (1986).
21. Yu Yao, Y.-F., *J. Catal.* **87,** 152 (1984).
22. Pierron, E. D., Rashkin, J. A., and Roth, J. F., *J. Catal.* **9,** 38 (1967).
23. Arnoldy, P., and Moulijn, J. A., *J. Catal.* **93,** 38 (1985).
24. Scheffer, B., Heijeinga, J. J., and Moulijn, J. A., *J. Phys. Chem.* **91,** 4752 (1987).
25. Personal communication with R. A. Dictor, Physical Chemistry Department, General Motors Research Laboratories, June 1988.
26. Kiss, J. T., and Gonzalez, R. D., *J. Phys. Chem.* **88,** 898 (1984).
27. Vis, J. C., van't Blik, H. F. J., Huizinga, T., van Grondelle, J., and Prins, R., *J. Catal.* **95,** 333 (1985).
28. Yao, H. C., Yu Yao, Y.-F., and Otto, K., *J. Catal.* **56,** 21 (1979).
29. Yates, D. J. C., Murrell, L. L., and Prestridge, E. B., *J. Catal.* **57,** 41 (1979).
30. van Zon, J. B. A. D., Koningsberger, D. C., van't Blik, H. F. J., and Sayers, D. E., *J. Chem. Phys.* **82,** 5742 (1985).
31. Robbins, J. L., *J. Phys. Chem.* **90,** 3381 (1986).
32. Solymosi, F., and Pasztor, M., *J. Phys. Chem.* **90,** 5312 (1986).
33. Solymosi, F., and Pasztor, M., *J. Phys. Chem.* **89,** 4789 (1985).
34. Bergeret, G., Gallezot, P., Gelin, P., Ben Taarit, Y., Lefebvre, F., Naccache, C., and Shannon, R. D., *J. Catal.* **104,** 279 (1987).
35. Fuentes, S., Vazquez, A., Perez, J. G., and Yacaman, M. J., *J. Catal.* **99,** 492 (1986).
36. Lee, C., and Schmidt, L. D., *J. Catal.* **101,** 123 (1986).